

**Time-dependent cavitation in a viscous fluid**

Vitaly A. Shneidman\*

*Department of Physics, New Jersey Institute of Technology, Newark, New Jersey 07102, USA*

(Received 1 June 2016; revised manuscript received 15 October 2016; published 1 December 2016)

Kinetics of nucleation and growth of empty bubbles in a nonvolatile incompressible fluid under negative pressure is considered within the generalized Zeldovich framework. The transient matched asymptotic solution obtained earlier for predominantly viscous nucleation is used to evaluate the distribution of growing cavities over sizes. Inertial effects described by the Rayleigh-Plesset equation are further included. The distributions are used to estimate the volume occupied by cavities, which leads to increase of pressure and eventual self-quenching of nucleation. Numerical solutions are obtained and compared with analytics. Due to rapid expansion of cavities the conventional separation of the nucleation and the growth time scales can be less distinct, which increases the role of transient effects. In particular, in the case of dominant viscosity a typical power-law tail of the quasistationary distribution is replaced by a time-dependent exponential tail. For fluids of the glycerin type such distributions can extend into the micrometer region, while in low-viscosity liquids (water, mercury) exponential distributions are short lived and are restricted to nanometer scales due to inertial effects.

DOI: [10.1103/PhysRevE.94.062101](https://doi.org/10.1103/PhysRevE.94.062101)**I. INTRODUCTION**

Cavitation, i.e., spontaneous formation of near-empty bubbles in a stretched liquid, belongs to a broad class of nucleation problems [1] with an enormous variety of scientific and technological applications. While often destructive [2], cavitation also offers a remarkable glimpse into the world of elementary particles via the bubble chamber [3,4] and has a direct link to such puzzling phenomena as sonoluminescence [5] and, more generally, to sonochemistry [6]. Recent advances in molecular dynamics (MD) studies of cavitation in nonmetallic [7–12] and metallic [13,14] fluids can clarify the elusive properties of the smallest subnano bubbles which provide a key boundary condition for the classical-type nucleation-growth equations and alternatively can reveal situations where the classical approach has to be reassessed.

Cavitation was the first nucleation problem which was treated starting from a purely macroscopic approach [15], with a huge variety of subsequent generalizations, including those to multi- [16–20] and infinite dimensions [21,22]. As compared to “regular” nucleation-growth problems controlled by the mass exchange between the nucleus and the metastable phase, the specifics of cavitation is that no material has to be exchanged between an empty cavity and the liquid [23]. Thus, the intuitively appealing microscopic picture of random addition of monomers to a nucleus (due to Farkas, Becker, and Döring) could not be applied to cavitation [24]. Also, the absence of mass exchange implies that growth of a cavity is limited only by viscosity and inertia of the liquid, and under certain conditions (as in a viscous fluid) this growth can be exponential, similar to growth of a “bubble” discussed in cosmological inflation models [3,25]. As a result, growth can occur on short time scales, comparable to those of time-dependent nucleation and the neglect of the latter (which is often justified in regular nucleation-growth situations) can lead to an error. The main intent of this paper is to demonstrate that time-dependent effects in classical cavitation indeed can be strong and can result in a qualitative change in the structure

of the distribution of growing bubbles. In addition, inertial effects which dominate for large cavities are included based on asymptotic analysis of the Rayleigh-Plesset hydrodynamic equation, which allows one to discuss potential experimental implications.

**II. BACKGROUND AND NOTATIONS****A. The Zeldovich equation**

The general steps of the classical approach to the nucleation problem involve the following. On the thermodynamic (Gibbs) stage, the minimal work  $W$  which is needed to form a nucleus of size  $R$  is evaluated. The maximum  $W_*$  is achieved at the critical size  $R = R_*$  and determines the dimensionless barrier to nucleation  $B = W_*/T \gg 1$ , with  $T$  being the thermal energy (Boltzmann constant is taken as 1). According to ideas of fluctuational thermodynamics, the nucleation rate can be estimated as  $I \sim \exp(-B)$  [26], although at this stage little can be said about the pre-exponential. Next, one considers deterministic (i.e., neglecting fluctuations) growth or decay of individual nuclei with a rate  $\dot{R}(R)$  which changes sign at  $R_*$ . The associated inverse time scale  $\tau^{-1} = d\dot{R}/dR$  at  $R = R_*$  eventually determines the kinetic part of the pre-exponential [15]. This completes the macroscopic part of the analysis and sets the background for the microscopic description which allows occasional rare nuclei to overcome the deterministic decay and to cross the barrier. Here one constructs a Fokker-Planck equation for  $f(R, t)$ , the distribution of nuclei over sizes. The diffusion coefficient  $D(R)$  in that equation is selected in such a way that the associated flux  $j = -D\partial f/\partial R + \dot{R}f$  is identically zero if the distribution coincides with the equilibrium one,  $f^{\text{eq}}(R) \sim \exp(-W/T)$ . For large  $B$  this requirement is equivalent to the Einstein relation in the  $R$  space:  $\dot{R} = -(D/T)dW/dR$  [15]. Formally, the Fokker-Planck equation (also known in this context as the “Zeldovich equation”) will resemble the continuous limit of the microscopically derived Becker-Döring equation and, similarly to the latter [27], can be solved exactly in the stationary limit. More appropriate, though, is the asymptotic solution for  $B \gg 1$  since the Zeldovich equation relies on this assumption

\*vitaly@njit.edu

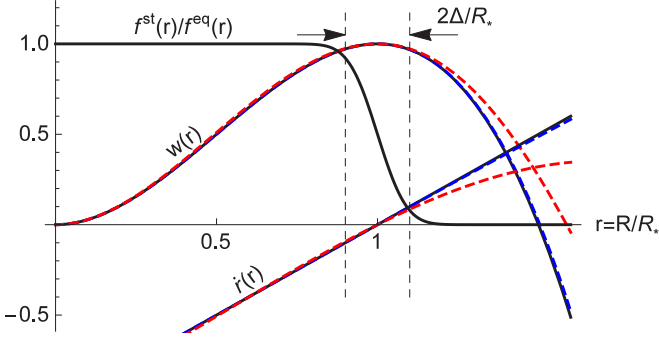


FIG. 1. Dimensionless representation of the main background functions.  $w(r) = 3r^2 - 2r^3$ —the scaled work  $W/W_*$  to form a cavity, and  $i(r) = r - 1$ —the growth rate, time scaled by  $\tau$  in Eq. (3), with no inertial effects (solid lines). Inertial corrections, which can be included iteratively at  $r \sim 1$ , are practically negligible for water and are visible but still small for mercury, as indicated by dashed lines for  $B \equiv W_*/T = 50$ . The vertical dashed lines locate the “critical region” where the change of the work  $W$  is comparable to thermal energy  $T$ . The stationary distribution of cavities over sizes  $f^{\text{st}}(r)$  drops from near-equilibrium  $f^{\text{eq}}(r) \sim \exp[-Bw(r)]$  to the left of the critical region to the growth asymptote  $f^{\text{st}}(r) \simeq I/i(r)$  to the right of that region,  $I$  being the nucleation rate. The corresponding solid line is Eq. (7).

from the start. In particular, the asymptotic stationary flux determines the pre-exponential of the nucleation rate [15] and, in contrast to its exact counterpart, allows time-dependent generalizations.

In textbooks, the classical approach is usually described in noncavitation terms, e.g., for nucleation in supersaturated solutions [28]. While this undoubtedly increases the amount of potential applications, some nontrivial hydrodynamic aspects of the cavitation problem are lost. In addition, evaluation of the work  $W$ , which can be a challenging task in other nucleation scenarios [29], is rather straightforward for the formation of an empty cavity in incompressible fluid considered in Ref. [15], allowing one to focus on kinetic effects. Thus, below we reproduce the Zeldovich equation closer to the original Ref. [15], somewhat generalizing the hydrodynamic stage of the derivation in order to better understand the connection with the macroscopic Rayleigh-Plesset (RP) equation for the growth and decay of cavities and to estimate the potential inertial effects (some aspects of the latter were also discussed in Refs. [19,30]).

Consider an isolated spherical cavity of radius  $R$  which grows (or collapses) with the rate  $\dot{R}$ . The velocity field around the cavity is radial and for incompressible fluid is given by  $u(r') = \dot{R}R^2/r'^2$ , where  $r' \geq R$  is the distance from the center of the cavity. The minimal work which is required to create the cavity, including the kinetic energy of the fluid, is then

$$W(R, \dot{R}) = 4\pi R^2 \sigma + \frac{4\pi}{3} R^3 P + 2\pi \rho R^3 \dot{R}^2 \quad (1)$$

(see the dimensionless bell-shaped solid and dashed curves in Fig. 1). In the above,  $\sigma$  is the surface tension,  $P < 0$  is the pressure, and  $\rho$  is the density;  $R_* = 2\sigma/(-P)$  is the critical size. The barrier to nucleation [saddle point in the  $(R, \dot{R})$  space] is still given by the Gibbs expression  $W_* = (4/3)\pi\sigma R_*^2$

and is unaffected by inertia. Although the absolute pressure  $|P|$  can be large, it is expected to be smaller than the Young modulus  $Y$  to ensure stability of the liquid on the atomic level. The condition  $|P| \ll Y$  also ensures that the limiting growth rate  $\dot{R}_\infty = \sqrt{2/3|P|/\rho}$  remains smaller than the speed of sound  $\sim \sqrt{Y/\rho}$ , which justifies the incompressibility assumption and which is satisfied for all liquids discussed below [31].

Dissipation  $dW/dt$  is due to viscosity  $\eta$ , and after integration of the Navier-Stokes equation over the bulk of the fluid can be expressed in general terms of a surface integral,  $-\eta \int (\nabla u^2) \cdot d\vec{f}$  [32], where  $d\vec{f}$  is the element of the surface. With the radial velocity field  $u(r')$  and a spherical surface the integrand is constant, so that one has [33]

$$dW/dt = -16\pi\eta R \dot{R}^2. \quad (2)$$

In a general situation this relation results in a nonlinear second-order RP equation for  $R(t)$  which cannot be solved exactly (see Sec. IID). Simplifications are possible since viscosity typically prevails at nucleation sizes  $R \lesssim R_*$  (see Fig. 1). For dominant viscosity the above dissipation relation leads to a first-order linear equation:

$$\dot{R} \simeq (R - R_*)/\tau, \quad \tau = 4\eta/(-P). \quad (3)$$

From here, small inertial corrections can be accounted for iteratively by replacing  $\dot{R}$  in Eq. (1) with the leading viscous term, Eq. (3). Since the work  $W$  is now uniquely determined by the size  $R$ , the nucleation problem becomes effectively one-dimensional. Inertial effects can become dominant at larger sizes during growth, but that is another stage which can be treated independently (see Sec. IV).

To describe nucleation, one constructs a Fokker-Planck equation for the distribution of cavities over sizes,  $f(R, t)$ :

$$\frac{\partial f}{\partial t} = -\frac{\partial j}{\partial R}, \quad j = -D f^{\text{eq}} \frac{\partial f}{\partial R} \frac{f}{f^{\text{eq}}}. \quad (4)$$

The quasiequilibrium distribution  $f^{\text{eq}}(R)$  is given by

$$f^{\text{eq}}(R) = A R_*^{-1} (R/R_*)^\nu \exp[-W(R)/T] \quad (5)$$

(the total number of cavities is evaluated per molecule, so that the constant  $A$  is dimensionless). The pre-exponential with some modest power index  $\nu$  is beyond the accuracy of the classical approach [28] but is often included into some of the nucleation problems [34–36] in order to improve its performance. As mentioned, the diffusion coefficient  $D(R)$  in Eq. (4) follows from the “Einstein relation”:  $T \dot{R} = -D dW/dR$  [15].

Comparing this to  $dW/dt = -16\pi\eta R \dot{R}^2$  one obtains

$$D(R) = T/(16\pi\eta R). \quad (6)$$

Note that the above expression is robust and holds regardless of the actual structure of  $W(R)$  (which can differ if, for example,  $\sigma = \sigma(R)$  is considered). The left boundary condition to Eq. (4) is taken as  $f(R_{\text{min}}) = f^{\text{eq}}(R_{\text{min}})$  at some small  $R_{\text{min}} \ll R_*$ , which usually indicates the minimal size where the macroscopic approach is still reasonable. On the right, one assumes a smooth transition to deterministic growth  $j \rightarrow \dot{R} f$  [or equivalently,  $f(R, t)/f^{\text{eq}}(R) \rightarrow 0$ ] for  $R - R_* \gg \Delta$ , with  $\Delta^{-2} = -1/(2T) d^2W/dR^2$  at  $R = R_*$ .

To construct an asymptotic stationary solution to Eq. (4), one linearizes its coefficients near  $R_*$ , which implies

$D(R) \simeq D(R_*) = \Delta^2/2\tau$ ,  $W(R) \simeq W_* - (R - R_*)^2/\Delta^2$ , and  $(R/R_*)^\nu \simeq 1$ . The resulting distribution, which is close to equilibrium below the critical region, is given by

$$f^{\text{st}}(R)/f^{\text{eq}}(R) = \frac{1}{2} \text{erfc}(z), \quad z = \frac{R - R_*}{\Delta}, \quad (7)$$

where  $\text{erfc}(z)$  is the ‘‘complementary error integral’’ [37] (see Fig. 1). The size-independent stationary flux (‘‘nucleation rate’’) is then [15]

$$I \simeq \Delta f^{\text{eq}}(R_*)/(2\tau\sqrt{\pi}), \quad (8)$$

which is  $Ae^{-B}/(\tau\sqrt{12\pi B})$  in the viscous limit. This does not contain  $R_{\min}$  or  $\nu$  (and the latter also does not enter into the time-dependent generalization described below), but those parameters can have an effect on the constant  $A$  once the normalization is specified (Appendix A). The distribution in the growth region  $R - R_* \gg \Delta$  is determined by

$$f^{\text{st}}(R) \simeq I/\dot{R}, \quad (9)$$

which coincides with the asymptote of Eq. (7) in the overlapping domain  $\Delta \ll R - R_* \ll R_*$ , but also is valid for large  $R \gg R_*$ . If viscosity at those sizes still dominates, Eq. (9) implies an  $R^{-1}$  tail of the distribution as follows from Eq. (3); a constant tail is expected when growth is limited by inertia with  $\dot{R} \simeq \text{const} = R_\infty$ .

## B. Transient nucleation

During the early stage of cavitation, with negligible volume of nucleated bubbles, the pressure (and thus the barrier and the critical size) are near constant, and the time dependence is due exclusively to transient effects. Although this interval is relatively short, it determines formation of the *largest* bubbles which can have a dominant effect on the increase of pressure and eventual termination of nucleation.

To streamline notations, let us switch to a dimensionless time  $t \rightarrow \int dt/\tau \simeq t/\tau(0)$  and size  $r = R/R_*(0)$ . The viscous growth rate, which is assumed to dominate, is just  $\dot{r} = r - r_*(t)$ , with  $r_*(0) = 1$  (see Fig. 1). The flux  $j$  and the nucleation rate  $I$  are multiplied by  $\tau$  and become dimensionless (although no new notations are used). Dimensional notations are restored at the end of Sec. IV when discussing potential relation to experiments. It is also convenient to define a double-exponential,

$$\phi(x) = \exp\{-\exp(-x)\}, \quad (10)$$

which appears in several, often unrelated, analytical expressions below.

For a large barrier  $B \gg 1$ , the time-dependent Eq. (4) can be solved using matched asymptotic (singular perturbation) technique [20,38,39]. A detailed description of the solution is presented in Appendix B; here we outline the major steps and the required results. First, Eq. (4) is rewritten in terms of the reduced distribution  $f(r,t)/f^{\text{eq}}(r)$  and the macroscopic growth rate  $\dot{r}$ . The small parameter  $\epsilon^2 = (\Delta/R_*)^2 = 1/3B$  appears explicitly as a coefficient which multiplies the second derivative. A Laplace transform with respect to time is applied to obtain an ordinary differential equation with a transition boundary layer near  $r = 1$ . This equation is solved using matched asymptotic expansion, which is from the same group of perturbation

methods as the WKB approximation [40]. Within the boundary layer, the  $\text{erfc}(z)$  of Eq. (7) is replaced by the ‘‘repeated error integral’’ [37] with the same argument  $z = (r - 1)/\epsilon$  and with the proportionality coefficient dependent on the Laplace index. The asymptote of the repeated error integral into the growth region,  $z \rightarrow \infty$ , allows one to determine the transform of the flux, which unlike the stationary case is  $r$  dependent. Inverting the Laplace transform at some  $r = r_0$  with  $\epsilon \ll r_0 - 1 \ll 1$ , one obtains the double-exponential time-dependence  $j(r_0, t)/I = \phi(x)$ , which is defined in Eq. (10) with [38]

$$x = t - t_i(x_0). \quad (11)$$

Here the ‘‘incubation time’’  $t_i(x_0)$  indicates the instant when the flux reaches  $1/e$  of its stationary value and is given by

$$t_i(x_0) = \ln(6B) + \ln(x_0 - 1) + \text{const}. \quad (12)$$

The constant is independent of the barrier and is determined by the properties of the integral  $\int dr/\dot{r}$  in the subcritical region. (For linear viscous growth and  $R_{\min} = 0$  this constant is zero—see Appendix B). The flux at  $r = r_0$  can be treated as the ‘‘nucleation rate,’’ implying that the shape of the flux does not change with growth and that it can be obtained at arbitrary size  $r > r_0$  as

$$j(r,t) = I\phi[t - t_i(r)], \quad (13)$$

with a shifted incubation time:

$$t_i(r) = t_i(r_0) + \int_{r_0}^r \frac{dr}{\dot{r}}. \quad (14)$$

The flux thus resembles a kind of ‘‘shock wave’’ with the front determined by the function  $\phi(x)$ , which propagates in the  $r$  space with the growth rate  $\dot{r}$ . As  $r \rightarrow 1$ , the growth integral  $\int dr/\dot{r}$  has the same logarithmic singularity as  $t_i(r_0)$ , so that the incubation time in Eq. (14) is  $r_0$  independent. This becomes obvious if the integral can be evaluated in elementary functions. In particular, for the viscous growth one has

$$t_i(r) = \ln[(r - 1)(1 - r_{\min})] + \ln 6B, \quad (15)$$

which generalizes a similar expression [39] for  $r_{\min} = R_{\min}/R_* > 0$ . Similarly, elementary expressions for  $t_i(r)$  are available for regular interface- and diffusion-limited growth [39]. If, on the other hand, the growth integral cannot be evaluated explicitly (as in case of inertial effects discussed in Sec. IV), one has to start with Eq. (14) and use some approximation when evaluating the growth integral. The approximation, however, should accurately reproduce the aforementioned singularity, otherwise the result will be sensitive to selection of  $r_0$ .

The distribution of growing cavities over sizes is given by direct analog of the stationary Eq. (9),  $f(r,t) = j(r,t)/\dot{r}$ , so that

$$f(r,t) = \frac{I}{\dot{r}} \phi[t - t_i(r)]. \quad (16)$$

The number of cavities with  $r > r_0$  corresponds to  $\Omega_0 = \int_{r_0}^{\infty} dr f(r,t)$ . It can be determined by integration of the transient flux over time [39]:

$$\Omega_0 = I \int_{-t_i}^{t-t_i} dx \phi(x) \simeq IE_1[\exp(t_i - t)], \quad (17)$$

with  $E_1$  being the exponential integral [37]. (The exponentially small contribution of the lower integration limit must be neglected within the accuracy of the asymptotic treatment.) At large  $t$  with  $t - t_i \gg 1$  the exponential integral of a small argument can be replaced by its logarithmic asymptote, and one has [39]

$$\Omega_0(r_0, t) = I[t - t_i(r_0) - \gamma]. \quad (18)$$

Here  $\gamma = 0.5772\dots$  is the Euler constant and  $t_i + \gamma$  is known as the ‘‘induction time’’ (or, the ‘‘time lag’’) of transient nucleation. Note that unlike the higher moments of the distribution described below, which are mostly determined by large sizes, the values of  $\Omega_0(r_0, t)$  are sensitive to the selection of  $r_0$  due to rapid increase of the distribution towards small  $r$ . Those values, nevertheless are convenient for scaled representation of the forthcoming results.

### C. Cavitation feedback

In a fixed volume, which corresponds to tensile strength experiments [2,41] or to typical MD simulations [10], the cavitation feedback is due to the volume  $\delta V$  occupied by expanding cavities. This results in the increase of the pressure

$$\delta P = Y \frac{\delta V}{v_L},$$

with  $Y$  being the aforementioned Young modulus and  $v_L$  the molecular volume of the fluid. Introducing  $v_* = (4/3)\pi R_*^3(0)$ , the volume of a critical bubble, one can relate  $\delta V$  to the dimensionless third moment:

$$\delta V = v_* \Omega_3, \quad \Omega_3 = \int_{r_1}^{\infty} dr r^3 f(r, t). \quad (19)$$

This type of closing condition is typical for the Becker-Döring equations [42]. Note that except for very early times, when  $\Omega_3$  is negligible, the integral is dominated by large  $r \gg 1$  and selection of the lower limit  $r_1 \sim 1$  should not matter (see a similar discussion in Ref. [43]). From  $B \propto P^{-2}$  one then estimates the change of the barrier

$$\delta B = \kappa B \Omega_3 \quad (20)$$

with a dimensionless  $\kappa = 2Yv_*/(-Pv_L)$ .

### D. Inertial effects

Let us introduce a characteristic ‘‘inertial size’’  $R_{\text{in}} = 8\eta^2/\rho\sigma$  and its dimensionless equivalent  $r_{\text{in}} = R_{\text{in}}/R_*$  which is assumed to be large (see Table I). The dimensionless work  $w \equiv W/W_*$  takes the form

$$w(r, \dot{r}) = 3r^2 - 2r^3 + \frac{3}{r_{\text{in}}} r^3 \dot{r}^2 \quad (21)$$

TABLE I. Parameters of the three liquids for  $B = 50$  at room temperature.

Liquid	$\tau$ (ns)	$R_*$ (Å)	$r_{\text{in}}$	$\kappa$
Water	$2.4 \times 10^{-2}$	8.4	136	2144
Mercury	$2.6 \times 10^{-3}$	3.5	9.41	186
Glycerin	34	8.4	$2.1 \times 10^8$	1172

(see Fig. 1), while the dissipation relation is given by

$$\dot{w} = -6r\dot{r}^2. \quad (22)$$

At nucleation sizes  $r \sim 1$  the inertial contributions are minor, of the order of  $1/r_{\text{in}}$ . Thus, one expects the general validity of the Zeldovich equation, Eq. (4)—otherwise its two-dimensional version in the  $(R, \dot{R})$  space could be required [19]. Growth, which involves large  $r \gg 1$ , however becomes different, affecting both the incubation time and the volume taken by the cavities (see Sec. IV). The full description of growth requires the solution of the Rayleigh-Plesset equation, which follows from the above equations for  $w$  and  $\dot{w}$ :

$$\dot{r} = r - 1 - \frac{r}{r_{\text{in}}} \left( r\ddot{r} + \frac{3}{2}\dot{r}^2 \right). \quad (23)$$

In order of appearance, the terms are due to viscosity, pressure, and curvature, and the last two terms can be labeled as ‘‘second-order’’ and ‘‘first-order’’ inertial terms, respectively. Since the equation does not allow an exact solution, various approximations are discussed in the literature [2]. In Sec. IV we utilize the condition  $r_{\text{in}} \gg 1$  and focus on approximations which allow a smooth extension of the incubation time  $t_i(r)$  from the viscosity-dominated region of small  $r \gtrsim 1$  towards large  $r \gg \sqrt{r_{\text{in}}}$  dominated by inertia.

### E. Numerics

In parallel to analytics, numerical solutions of the discretized version of Eqs. (4)–(6) (without inertial effects) complemented by the closing Eq. (20) were obtained using MATHEMATICA 10. The nucleation and the growth regions were typically linked at  $r_0 = 2$ , with a similar value used for  $r_1$  in Eq. (19), and the insensitivity of the results to the selection could be verified operationally. The dominant dimensionless parameter is the barrier  $B = B(0)$  and two extreme values of ‘‘small’’  $B = 20$  and ‘‘large’’  $B = 50$  were considered. This lead to an enormous ( $\sim 10^{13}$ ) span of the nucleation rates and to a noticeable change in the weak  $B$ -dependent functions, such as  $\ln B$  or  $B^{1/3}$ , which allowed the testing of some of the asymptotic scaling relations. The anticipated input of other parameters is less dramatic, and they were mostly held unchanged in simulations of Sec. III intended to assess analytics:  $\kappa A = 0.01B$ ,  $\nu = 0$ , and  $r_{\text{min}} = 0.1$ .

Once inertial effects were included, numerics was used to integrate the Rayleigh-Plesset equation. This was done in order to verify some of the analytical approximations and to generate results on incubation times, distributions, and metastable-state life times for parameters related to several common fluids (see Table I). One should keep in mind, though that the classical expression for the nucleation rate  $I$ , Eq. (A2), used in those calculations often underestimates experimental values and leads to absolute pressures  $|P|$  which are much higher than observable [2]. Thus, the physical parameters which can be inferred from Table I should be treated as tentative. In particular, identical values of  $\sigma \simeq 0.07 \text{ N/m}$  are used for both water and for glycerin, which results in similar thermodynamics of nucleation and highlights the differences due to kinetic competition between the viscous and the inertial effects.

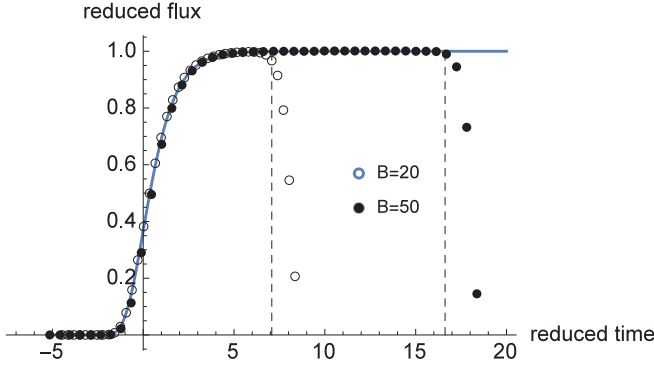


FIG. 2. Reduced flux  $j(r,t)/I(0)$  at  $r = 2$  as a function of reduced time  $t - t_i(r)$  for two different initial barriers  $B$ . Solid line: Eqs. (13) and (15). Symbols: Numerics. The vertical dashed lines indicate quenching of nucleation by growing cavities, Eq. (25) for  $B = 50$  (right) and  $B = 20$  (left).

### III. RESULTS

Typical time dependences of the nucleation flux  $j(r_0, t)$  in a viscous fluid are shown in Fig. 2. During early times the flux passes through a transient stage and approaches the quasistationary value  $I \simeq I(0)$ . This value persists up to a certain nucleation time  $t_n$  (defined below) until the negative pressure is increased by expanding cavities and nucleation is quenched. Compared to regular nucleation problems with a power-law growth, where the nucleation time is exponentially large, in the case of cavitation this time is much shorter, approximately only a linear function of the barrier, due to rapid increase of the size of the growing cavities. Also, in contrast to aforementioned regular problems where depletion of the metastable phase leads to a *gradual* reduction of the rate [43], in the present case the transition to near-zero flux at  $t \gtrsim t_n$  is sharp, which expands the domain of applicability of the transient solution.

As seen from Fig. 2, the Eqs. (13) and (15) are accurate: shifting the time by  $t_i(r)$  brings the early (transient) data onto the parameter-free master curve given by Eq. (10). Thus, the solution can be used to find the distribution of growing cavities over sizes in Eq. (16).

From here, the problem can be treated iteratively. The above distribution allows one to obtain the leading approximation for the third moment. Without restrictions imposed by inertial effects, the growth rate is just  $r - 1$ , and particles grow exponentially with time. One has

$$\Omega_3(t) \approx 2I \exp\{3(t - \ln[6B(1 - r_{\min})])\}. \quad (24)$$

The logarithmic term is large, and transient nucleation effects are important as long as growth is given by Eq. (3). In fact, the neglect of such effects would leave an undetermined factor  $O(1)$  since the stationary solution alone does not provide the initial size  $r_0$  of nucleated cavities. (In contrast, the transient distribution is  $r_0$  independent for a properly selected  $\Delta/R_* \ll r_0 - 1 \ll 1$ ; see Appendix B). The overall nucleation time  $t_n$  can be estimated by substituting the increased barrier  $B(t) = B(0) + \delta B$ , with  $\delta B$  determined by Eqs. (20) and (24), into

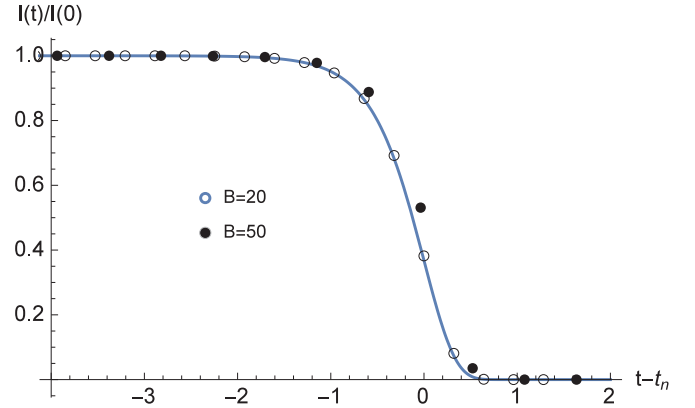


FIG. 3. Reduced adiabatic nucleation rate from Eqs. (10) and (25) (solid line) and from numerics (symbols). Note the large-time scaling once time  $t$  is reduced by the nucleation time  $t_n$ .

the adiabatic Eq. (8). Neglecting  $r_{\min}$ , one obtains

$$I(t)/I(0) = \phi[3(t_n - t)], \quad (25)$$

with

$$t_n \simeq -\frac{1}{3} \ln \frac{I\kappa}{108B^2}. \quad (26)$$

This is illustrated in Fig. 3.

To explore the tail of the transient distribution at  $r \gg 1$  we scale it with a characteristic size  $\bar{r}(t)$  at  $1 \ll t \lesssim t_n$

$$\begin{aligned} \bar{r}(t) &= \left(\frac{\Omega_3}{\Omega_0}\right)^{1/3} \approx \frac{e^t}{6B} \left(\frac{\tilde{t}}{2}\right)^{-1/3}, \\ \tilde{t} &= t - \ln(6B) - \ln(r_0 - 1) - \gamma. \end{aligned} \quad (27)$$

From Eqs. (15) and (16) one obtains the tail of the normalized distribution  $\tilde{f}(l,t) = (\Omega_0)^{-1} \bar{r} f(r,t)$  with the scaled size  $l = r/\bar{r}$ :

$$\tilde{f}(l,t) \simeq \frac{1}{l\tilde{t}} \exp\left[-l\left(\frac{2}{\tilde{t}}\right)^{1/3}\right]. \quad (28)$$

This is shown by solid lines in Figs. 4 and 5 together with the scaled numerical data represented by symbols. The quasi-steady-state distributions, scaled using the same (numerical)

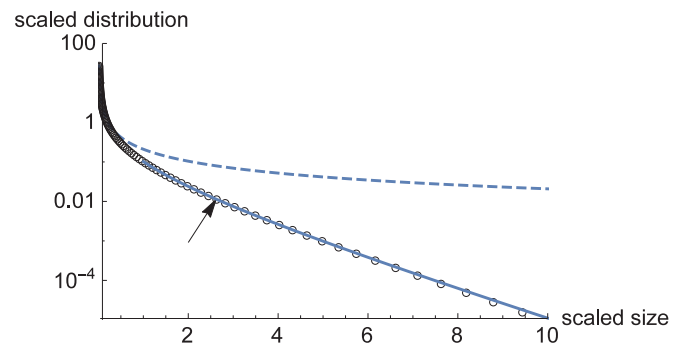
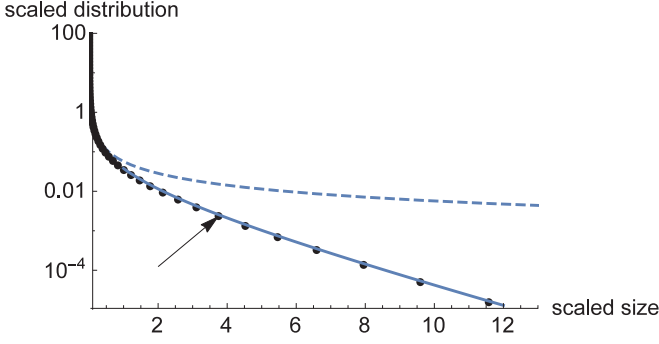


FIG. 4. Exponential tail of the scaled distribution in Eq. (28) at  $t \approx t_n$  for the initial barrier  $B = 20$  (solid line). Symbols: Numerics. he arrow indicates sizes which give maximum contribution to the nucleated volume. Dashed line: Tail of the quasi-steady-state distribution, a power law.

FIG. 5. Same as in Fig. 4 for initial barrier  $B = 50$ .

values of  $\Omega_0$  and  $\Omega_3$ , are indicated by the dashed lines. Note that the quasistationary power-law tail has been replaced by an exponential, which is the first main result of the present paper. The arrows in Figs. 4 and 5 indicate the maximums of  $l^3 \tilde{f}(l, t)$  achieved at  $l_m \simeq 2^{2/3} \tilde{t}^{1/3}$ , close to  $B^{1/3}$  if  $t \approx t_n$  (which is the upper limit of applicability). The values of  $l_m$  determine the sizes of bubbles which are responsible for termination of nucleation; huge deviations at those sizes from the quasistationary distribution are noteworthy.

#### IV. ESTIMATIONS OF INERTIAL EFFECTS AND DISCUSSION

For small inertial contributions, one can insert the viscous growth rate  $\dot{r} = r - 1$  into the work  $w(r)$  given by Eq. (21). This will modify the off-critical growth once the dissipation relation  $\dot{w} = -6r\dot{r}^2$  is used. One obtains the leading correction

$$\dot{r} = (r - 1) \left[ 1 + (3 - 5r) \frac{r}{2r_{\text{in}}} \right], \quad r \ll \sqrt{r_{\text{in}}}, \quad (29)$$

where  $r_{\text{in}}$  is defined in Sec. II D. The time scale  $\tau' = 1/(d\dot{r}/dr)$  at  $r = 1$  is given by  $1/(1 - 1/r_{\text{in}})$ . To evaluate the correction to the incubation time  $t_i(r)$  one isolates the singular term in the inverse growth rate

$$\frac{1}{\tau' \dot{r}} \simeq \frac{1}{r - 1} + \mu(r),$$

with  $\mu(r) = (2 + 5r)/2r_{\text{in}}$ . The singular term leads to Eq. (15) multiplied by  $\tau'$  (which is close to 1 and will be henceforth ignored). Evaluation of the integrals involving  $\mu(r)$ , Eq. (B14), gives the correction

$$\delta t_i(r) = \frac{1}{4r_{\text{in}}} [5(r^2 + r_{\text{min}}^2) + 4(r + r_{\text{min}}) - 18]. \quad (30)$$

At nucleation sizes  $r \sim 1$  the corrections are minor due to large values of  $r_{\text{in}}$  (see Table I). On the other hand, inertial effects become important with growth—note the quadratic term in Eq. (30)—and prevail for  $r \gtrsim \sqrt{r_{\text{in}}}$ . Here one needs the RP equation, Eq. (23). Considering dominance of various terms at different sizes in the growth region (see Appendix B), one obtains the following asymptotic dependence for the growth time  $t_{gr}(r_0, r) = \int_{r_0}^r dr/\dot{r}$  from a near-critical size  $r_0 \rightarrow 1^+$  to a large size  $r \gg \sqrt{r_{\text{in}}} \gg 1$ :

$$t_{gr}(r_0, r) \simeq \frac{r}{\dot{r}_{\infty}} + \ln \frac{r^{3/4} r_{\text{in}}^{1/8}}{r_0 - 1} + \text{const}, \quad (31)$$

with

$$\dot{r}_{\infty} = \sqrt{\frac{2r_{\text{in}}}{3}}. \quad (32)$$

The constant in Eq. (31) is  $r_0$  and  $r_{\text{in}}$  independent and can be obtained numerically as  $-0.6$ . Note that as  $r_0 \rightarrow 1$  the singularity in Eq. (31) is similar and opposite in sign to the one in Eq. (15). Thus, in accord with Eq. (14) the inertial incubation time  $t_i^{\text{in}}(r) = t_i(r_0) + t_{gr}(r_0, r)$  is  $r_0$  independent:

$$t_i^{\text{in}}(r) \simeq \frac{r}{\dot{r}_{\infty}} + \frac{3}{4} \ln \frac{r}{\sqrt{r_{\text{in}}}} + \ln(6B\sqrt{r_{\text{in}}}) - 0.6. \quad (33)$$

Here small inertial corrections due to  $\delta t_i(r_0) \sim 1/r_{\text{in}}$  are not included since that would exceed the accuracy of the asymptotic treatment; similarly, the small  $r_{\text{min}} \ll 1$  is dropped from Eq. (15). Equation (33) represents the second main result of this work.

To describe the entire growth region, at small  $r$  one can consider mostly viscous growth described by Eq. (15) with minor inertial corrections (30) and then, at larger sizes, switch to Eq. (33) dominated by inertia. In order to minimize the discontinuity, the transition should be made around  $0.3\sqrt{r_{\text{in}}}$ , so that the interpolating incubation time, which replaces the logarithmic  $t_i(r)$  in Eqs. (13) and (16) is given by

$$t_i(r) + \delta t_i(r), \quad 1 < r \leq 0.3\sqrt{r_{\text{in}}}, \quad (34)$$

$$t_i^{\text{in}}(r), \quad r > 0.3\sqrt{r_{\text{in}}}.$$

Alternatively, one can deduce  $t_{gr}(r_0, r)$  from the time dependence of the size of a growing cavity  $r(t)$  based on numerical integration of the RP equation. Initial conditions are taken as  $r(t_0) = r_0 = 2$  and  $\dot{r}(t_0) = r_0 - 1$ , with  $t_0 = t_i(r_0) + \delta t_i(r_0)$ . Figure 6 shows comparison of numerics (solid lines) and Eq. (34) (dashed) for parameters of several common liquids with  $B = 50$ . Note the transition from logarithmic dependence at all sizes, which is characteristic for viscous growth of cavities in glycerin, to more conventional linear dependence at  $r \gtrsim \sqrt{r_{\text{in}}}$  for inertial growth in water and mercury. In the

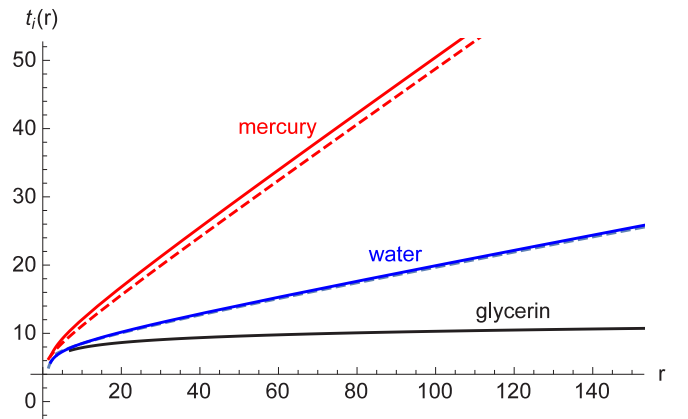


FIG. 6. Incubation time including inertial effects in growth for  $B = 50$ . All times are scaled with respective  $\tau$  and sizes with respective  $R_*$  (see Table I). Solid line: From integration of Rayleigh-Plesset equation. Dashed line: From interpolating Eq. (34). For the sizes considered, inertial effects are invisible for glycerin at room temperature, where the  $r$  dependence remains logarithmic.

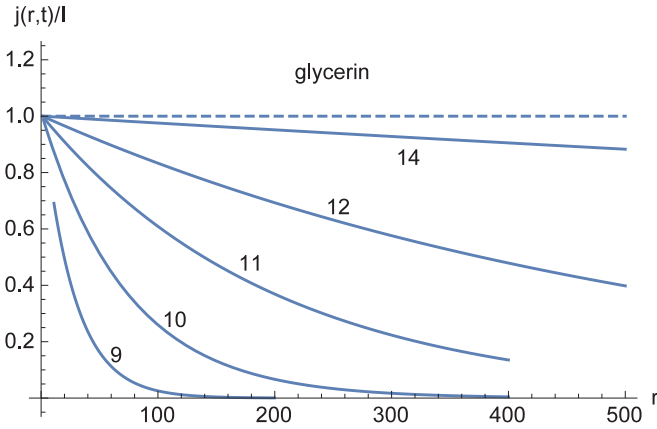


FIG. 7. Transition to quasistationary flux in the case of viscous growth. The curves are labeled by dimensionless time  $t$  (in units of  $\tau \approx 34$  ns). The size is scaled by the critical size  $R_* \approx 8.4 \text{ \AA}$  for  $B = 50$ .

latter case accuracy of the asymptotic approximation is lower since  $r_{in}$  is smaller, indicating stronger inertial effects.

To demonstrate the qualitative difference of the resulting transient distributions of cavities over sizes, consider Figs. 7 and 8 which present the drift fluxes  $j(r,t) = f(r,t)\dot{r}$  (fluxes are more convenient for visual comparison since they tend to an  $r$ -independent constant in steady state, regardless of the growth mechanism). The distributions are given by Eqs. (13) and (34). In the viscous case one has broad exponential distributions, with a time-dependent slope and without a well-defined front. Conversely, in the inertial case one observes a sharp transition to steady state via propagation of a “shock wave” in the  $r$  space, with a narrow double-exponential front, similar to the one in conventional interface-limited nucleation and growth [39].

Existence of the distributions of either type is limited by the lifetime of a metastable state, or the nucleation time  $t_n$  which can be estimated from

$$\kappa B \Omega_3(t_n) \sim 1. \quad (35)$$

For viscous growth with exponential  $\Omega_3(t)$  this gives Eq. (26). In the opposite, inertial limit one has

$$\Omega_3^{in}(t) \simeq \frac{1}{4} I \dot{r}_\infty^3 t^4, \quad (36)$$

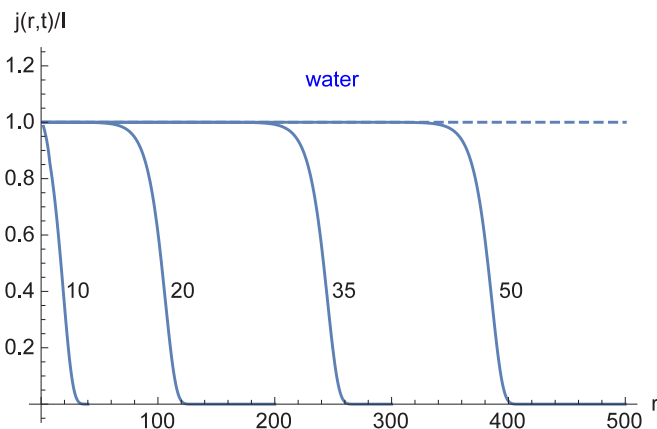


FIG. 8. Same as in Fig. 7 but for inertial growth. Time is scaled by  $\tau \approx 0.024$  ns; size is scaled by  $8.4 \text{ \AA}$ .

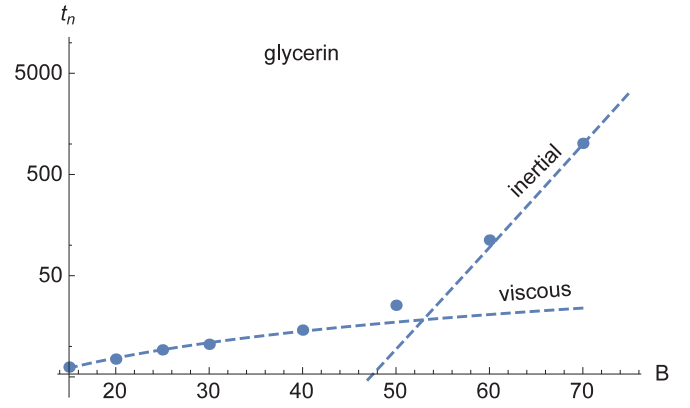


FIG. 9. Estimations of the dimensionless nucleation time (in units of  $\tau \approx 4.8\sqrt{B}$ , ns) as a function of the initial barrier  $B$ . Symbols: From Eq. (35) with numerical integration of the distribution of nuclei over sizes. Dashed lines:  $B/3$  and Eq. (37) for viscous and inertial growth, respectively.

which is the cavitation equivalent of the Kolmogorov-Avrami expression. With the classical estimation of the dimensionless flux  $I$  (see Appendix A) and with  $\dot{r}_\infty$  given by Eq. (32) one obtains

$$t_n^{in} \simeq [3\pi^2 / (2\kappa^2 r_{in}^3)]^{1/8} B^{-1/2} e^{B/4}. \quad (37)$$

In the intermediate cases,  $\Omega_3$  in Eq. (35) can be obtained by numerical integration of the distribution given by Eqs. (13) and (34). An additional requirement for the applicability of the results is the large overall number of nuclei in the system under consideration:

$$N_A I t_n \gg 1.$$

Here the Avogadro number  $N_A$  should be replaced by the actual number of monomers in the system, if those numbers are significantly different (as in MD simulations). Considering, for the sake of estimation,  $N_A \sim 10^{24}$  and only the leading terms in  $B$ , one obtains  $B \lesssim 58$  and  $B \lesssim 76$  for viscous and inertial growth, respectively, and for larger barriers nucleation should be treated statistically [44].

With the above restrictions in mind, typical nucleation times  $t_n$  are illustrated in Figs. 9 and 10. Note that smaller barriers favor viscous cavitation, while for large barriers the inertial

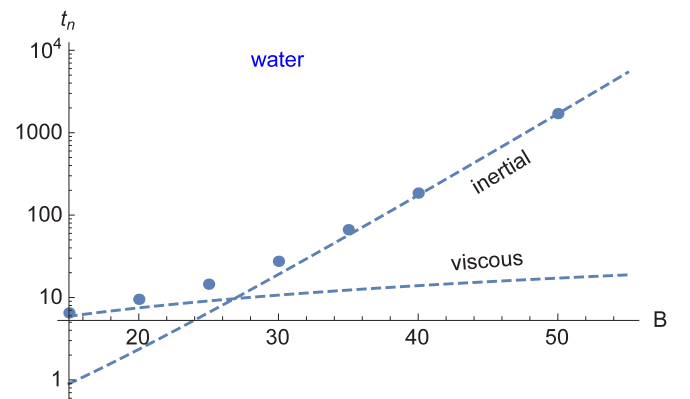


FIG. 10. Same as in Fig. 9 for water with  $\tau \approx 3.4\sqrt{B}$ , ps, and with predominantly inertial growth.

effects in growth are dominant since there are fewer cavities and they have to grow to larger sizes in order to have an effect.

To discuss potential observability of the time-dependent exponential distributions of cavities over sizes, which are expected for viscous nucleation and growth, we switch back to dimensional variables. The sizes  $R$  should be limited by  $R \lesssim R_* \sqrt{r_{in}}$ , which is the “viscous domain” with minor inertial effects. For room-temperature glycerin this extends to optically visible sizes (see Table I), so it could be possible to observe such distribution directly. The time limitation can produce a more serious challenge and is determined by the duration of the metastable state, about  $\tau B/3 \sim 10^{-7}$ – $10^{-6}$  s; lowering of temperature would increase this time which is proportional to viscosity. On the other hand, for a low-viscous liquid, such as water, the limiting size  $R$  is only one order above  $R_*$  while time is restricted by  $(1/2)\tau \ln(r_{in}) \lesssim 1$  ns. (The metastable state will persist at larger times, but then the distributions will be indistinguishable from conventional  $f^{st}(R) \propto R^{-1}$  and  $f^{st}(R) \propto R^0$  in the viscous and inertial domains, respectively, with transition to steady state described by a sharp double-exponential front). Despite the difficulty of the detection of such short-lived distributions, the above analysis can still be useful in that it allows one to select the size  $R_0$  from which growth starts as much larger than  $R_*$ , with the nucleation rate at  $R_0$  accurately described by Eqs. (10) and (13); the incubation time  $t_i(R_0)$  is given by Eq. (34). Subsequent integration of the Rayleigh-Plesset equation for growth of nucleated cavities is then simplified due to the condition  $R_0 \gg R_*$ , and the resulting distributions will be  $R_0$  independent. This can be of help in applied problems when cavitation is part of a more complex hydrodynamics [2].

In summary, both viscous and inertial effects in nucleation and growth of cavities were considered, and analytical approximations for size-dependent incubation times were derived. Typically, inertial effects are minor for nucleation sizes of the order of the critical size, but become dominant with the growth of cavities. The type of evolution to be considered, viscous vs inertial, depends on whether the corresponding sizes are reached before nucleation is quenched. In case the metastable state survives the viscous stage and the inertial growth becomes dominant (as in water), the distributions of cavities over sizes resemble those for regular interface-limited nucleation, with a long near-constant tail which is sharply terminated due to brief transient nucleation. Exponential distributions predicted by this study are still present, but they are short lived and are restricted to nanometer sizes. In contrast, in a viscous fluid such as glycerin, growth is exponential, which shortens the lifetime of the metastable state relative to the transient nucleation time scale. The resulting exponential distributions persist during the entire nucleation stage and can extend into the domain of micrometers. Most likely, however, the easiest way to observe such distributions would be in MD simulations where there are little restrictions on the smallest times and sizes which can be considered.

#### APPENDIX A: PRE-EXPONENTIAL IN THE QUASIEQUILIBRIUM DISTRIBUTION

Consider the normalization constant  $A$  in Eq. (5). Asymptotically, the contribution of the smallest bubbles to their

overall number ( $N$  per molecule of the fluid) is expected to dominate. Neglecting the cubic terms in Eq. (1) and assuming no bubbles with  $R < R_{min}$ , one obtains

$$A \approx 2N(3B)^{(v+1)/2} / \Gamma \left[ \frac{v+1}{2}, (R_{min}/\Delta)^2 \right], \quad (\text{A1})$$

where  $\Gamma(a,b)$  is the incomplete Gamma function [37]. (The presence of  $\Delta$ —the width of the near-critical region which is outside of the main integration domain—is coincidental.) In MD simulations the value of  $N$  can be measured directly [12], otherwise  $N \sim 1$  for a small  $R_{min}$  can be assumed. [If, instead of  $N$  the “free volume”  $v^f$  is known, a similar estimation for  $A$  can be used with  $v$  replaced by  $v+3$  and  $N$  replaced by  $(4\pi/3)v^f/v_L$ .] Although the factor  $A$  appears singular when phase equilibrium with  $B \rightarrow \infty$  is approached, the *full* pre-exponential of Eq. (5), which contains a compensating term,  $R_*^{-v-1}$ , remains finite.

It is often assumed [28] that  $R_{min} \approx 0$  and  $v = 2$ , which ensures a constant pre-exponential in the equilibrium distribution over the volumes of bubbles,  $f^{eq}(v) = f^{eq}(R)dR/dv$ . In that case one has

$$A = 12N\sqrt{3/\pi}B^{3/2}, \quad (\text{A2})$$

with the stationary nucleation rate per molecule of the viscous fluid

$$I = \frac{6}{\pi\tau}NB e^{-B} \simeq \frac{2N}{\eta} \sqrt{\frac{3B\sigma^3}{\pi T}} e^{-B}. \quad (\text{A3})$$

If, on the other hand,  $R_{min} \gg \Delta$ , then Eq. (A1) leads to

$$A \sim 2N(3B)^{(v+1)/2} (R_{min}/\Delta)^{1-v} \exp[(R_{min}/\Delta)^2], \quad (\text{A4})$$

which is exponentially large. This is notable since the classical rate  $I$  from Eq. (A3) with  $N \sim 1$  typically underestimates the experimental values. In fact, for  $R_{min} \gg \Delta$  the normalization integral can be obtained somewhat more accurately, without neglecting the cubic term. Due to dominance of the exponential term on the lower limit of the asymptotic normalization integral  $\int dR f^{eq}(R)$  one has

$$I = \frac{N}{\sqrt{\pi}} \frac{-\dot{R}_{min}}{\Delta} \frac{D(R_*)}{D(R_{min})} \left( \frac{R_*}{R_{min}} \right)^v \exp \frac{W(R_{min}) - W(R_*)}{T}. \quad (\text{A5})$$

The reduction of the barrier by the work required to form a nucleus of the smallest size  $R_{min}$  is well known, and corresponding expressions for the nucleation rate are often referred to as “adjusted classical theory.” The values of  $\dot{R}_{min}$  and  $D(R)$  follow from Eqs. (3) and (6), respectively.

#### APPENDIX B: TRANSIENT SOLUTION OF THE VISCOUS ZELDOVICH EQUATION [38,39] AND ITS EXTENSION FOR INERTIAL EFFECTS

Let us define a small parameter  $\epsilon = \Delta/R_* = 1/\sqrt{3B}$  and rewrite the Zeldovich equation, Eq. (4), in terms of dimensionless size  $r = R/R_*$  and reduced distribution  $q(r,t) = f(r,t)/f^{eq}(r)$ :

$$\frac{1}{2}\epsilon^2 \frac{\partial}{\partial r} \frac{D}{D_*} \frac{\partial q}{\partial r} + \dot{r} \frac{\partial q}{\partial r} = \frac{\partial q}{\partial t}. \quad (\text{B1})$$

At this point, general  $\epsilon$ -independent known functions  $\dot{r}(r)$  and  $D(r)/D_*$  are assumed in Eq. (B1), with  $\dot{r}(1) = 0$  and  $D(1)/D_* = 1$ . Time  $t$  is measured in units of  $\tau$ , so that  $d\dot{r}/dr = 1$  at  $r = 1$ . Introducing the Laplace transform (LT)

$$Q(r,s) = \int_0^\infty dt q(r,t) e^{-st},$$

one obtains an ordinary differential equation:

$$\frac{1}{2}\epsilon^2 \frac{d}{dr} \frac{D}{D_*} \frac{dQ}{dr} + \dot{r} \frac{dQ}{dr} = Qs, \quad (\text{B2})$$

where  $q(r,0) = 0$  is assumed. The left boundary condition is given by

$$Q(0,s) = 1/s,$$

where for simplicity of notation  $r_{\min}$  is treated as zero, similarly to Refs. [38,39]; arbitrary  $0 \leq r_{\min} < 1$  will be reintroduced into the final answers. We now use the method of matched asymptotic expansions [40], constructing an ‘‘outer’’ solution of the first-order equation (in neglect of  $\epsilon$ ) in the subcritical region and an ‘‘inner’’ solution of the linearized second-order equation describing the transition boundary layer near  $r = 1$ .

One has the outer solution at  $0 \leq r < 1$  (with  $1 - r \gg \epsilon$ ), which satisfies the left-hand boundary condition

$$Q^{\text{out}}(r,s) = \frac{1}{s} \exp \left[ s \int_0^r \frac{dr}{\dot{r}} \right] \quad (\text{B3})$$

(in time variables, the outer solution  $q^{\text{out}}(r,t) = \theta(t + \int dr/\dot{r})$  would correspond to a sharp front, which moves upstream, against the deterministic decay in accord with ‘‘microscopic reversibility’’). Near  $r = 1$  the integral diverges, and the asymptote is given by

$$Q^{\text{out}}(r \rightarrow 1,s) \sim \frac{1}{s} e^{sC} (1-r)^s, \quad C = \int_0^1 dr \left( \frac{1}{\dot{r}} - \frac{1}{r-1} \right). \quad (\text{B4})$$

The inner region is described in terms of a ‘‘stretched variable,’’  $z = (r-1)/\epsilon$ ,

$$\frac{d^2 Q}{dz^2} + 2z \frac{dQ}{dz} - 2sQ = 0, \quad |z| \ll \frac{1}{\epsilon}, \quad (\text{B5})$$

with the solution

$$Q^{\text{in}}(r,s) = \frac{1}{2} K(s) i^s \text{erfc}(z). \quad (\text{B6})$$

Here  $i^s \text{erfc}(z)$  is the ‘‘repeated error integral’’ [37] with asymptotes  $2(-z)^s / \Gamma(s+1)$  for  $z \rightarrow -\infty$  and  $(2/\sqrt{\pi}) e^{-z^2} (2z)^{-s-1}$  for  $z \rightarrow +\infty$  (and the second linearly independent solution  $i^s \text{erfc}(-z)$  has a wrong asymptote as  $z \rightarrow \infty$ ). The domains of applicability of the inner and outer solutions overlap at  $\epsilon \ll 1 - r \ll 1$ , which allows one to evaluate  $K(s)$  from matching the asymptotes

$$K(s) = \Gamma(s) e^{sC} \epsilon^s, \quad (\text{B7})$$

where  $\Gamma(s)$  is the Gamma function.

The LT of the flux is given by

$$J^{\text{in}}(r,s) = -I\sqrt{\pi} e^{z^2} \frac{dQ}{dz} = IK(s) \frac{\sqrt{\pi}}{2} e^{z^2} i^{s-1} \text{erfc}(z), \quad (\text{B8})$$

with an asymptote towards the growth region

$$J(r,s) = IK(s) \left( 2 \frac{r-1}{\epsilon} \right)^{-s}, \quad r-1 \gg \epsilon. \quad (\text{B9})$$

For the inversion of the LT we use

$$j(r,t) \simeq \sum'_s e^{st} \text{Res } J(r,s), \quad (\text{B10})$$

where the prime indicates summation over residues located in the finite part of the complex  $s$  plane. (Note that the formula is asymptotic, thus at  $t = 0$  an asymptotic, not necessarily an exact, zero is expected). The location of residues coincide with those of  $\Gamma(s)$  at finite  $s$ , with  $\text{Res } \Gamma(s) = 1/(-s)!$  at  $s = 0, -1, -2, \dots$  [37]. Performing the summation explicitly one obtains [38]

$$j(r,t) = I \exp\{-\exp[t_i(r) - t]\}, \quad (\text{B11})$$

which is  $I\phi(t - t_i)$  with  $\phi(x)$  defined in Eq. (10). The ‘‘incubation time’’ is given by [38]

$$t_i(r) = \ln \frac{2}{\epsilon^2} - C + \ln(r-1). \quad (\text{B12})$$

Equations (B11) and (B12) determine the nucleation rate at some ‘‘initial size’’  $r = r_0 > 1$  with  $r_0 - 1 \ll 1$ . For viscous growth with  $\dot{r} = r - 1$  at any size (and not only near  $r \approx 1$ ) there are no restrictions on  $r$  from above, and with  $C = 0$  Eq. (B12) is valid for the entire growth region [39]. For a nonlinear  $\dot{r}(r)$ , one can extend Eq. (B12) (with  $r$  replaced by  $r_0$ ) via increasing  $t_i(r_0)$  by the growth time  $\int_{r_0}^r dr/\dot{r}$ , as in Eq. (14). Since the growth integral has a singularity  $-\ln(r_0 - 1)$  as  $r_0 \rightarrow 1$ , the result will be  $r_0$  independent, indicating asymptotically smooth matching of the nucleation and the growth regions. Two alternative explicit representations of the final result are possible [39], and we use the one with isolated  $\epsilon$  dependence,

$$t_i(r) = \ln \frac{2}{\epsilon^2} + \mathbf{P} \int_0^r \frac{dr}{\dot{r}} - 2C, \quad (\text{B13})$$

where  $\mathbf{P}$  indicates the principal value of the integral.

The above expression can be used as a starting point to include inertial effects, which is the novel part of the present study. In the nucleation region such effects are small, and result only in the modification of the functional form of  $\dot{r}(r)$  (see Sec. IV). It is convenient then to represent the result as a correction to the case with viscous (linear) growth by isolating the singular part of the inverse rate:

$$\frac{1}{\tau' \dot{r}} = 1/(r-1) + \mu(r),$$

with  $\mu(r)$  which is regular at  $r = 1$  and  $\tau' = 1/(d\dot{r}/dr)$  at  $r = 1$ . The singular part is the only one which requires the principal value integration in Eq. (B13), which leads to Eq. (B12) (with  $C = 0$ ), multiplied by  $\tau'$ . The regular integration of  $\mu(r)$  gives the correction  $\delta t_i$  with

$$\frac{1}{\tau'} \delta t_i(r) = \int_1^r dr \mu(r) - \int_0^1 dr \mu(r). \quad (\text{B14})$$

For a nonzero  $r_{\min}$  the lower integration limit in the second integral should be adjusted accordingly. In the cases of interface- and diffusion-limited growth, respectively,  $\mu(r)$  is

given by 1 and by  $1 + r$ ; evaluation of the integrals then leads to known polynomial corrections to the logarithmic equation, Eq. (B12) [39]. In the case of inertial effects in the cavitation problem, the function  $\mu(r)$  is a linear combination of the aforementioned expressions, and the resulting modifications of the incubation time are presented in Sec. IV.

To describe the entire growth region, one needs to consider the full RP equation, Eq. (23). Although this equation cannot be solved exactly, certain asymptotic insight can be obtained from the condition  $r_{\text{in}} \gg 1$  (i.e., the inertial effects are assumed to be minor at the nucleation sizes, although they dominate when the size becomes large). Let us rescale the size  $r$  as  $y = rr_{\text{in}}^{-\alpha}$  with yet unknown power  $\alpha$ . The RP equation takes the form

$$\dot{y}r_{\text{in}}^{\alpha} = yr_{\text{in}}^{\alpha} - 1 - r_{\text{in}}^{3\alpha-1}y\left(\ddot{y} + \frac{3}{2}\dot{y}^2\right). \quad (\text{B15})$$

There are two solutions,  $\alpha = 0$  and  $\alpha = 1/2$ , when several dominant terms balance each other. The former case corresponds to dominance of viscous and curvature effects, with a solution  $r - 1 \sim (r_0 - 1)e^t$ . The case  $\alpha = 1/2$  corresponds to negligible curvature effects with viscous and inertial terms balancing each other:

$$\dot{y} = y - y\left(y\ddot{y} + \frac{3}{2}\dot{y}^2\right). \quad (\text{B16})$$

At small  $t$  this equation has a solution  $y \sim e^t(r_0 - 1)/\sqrt{r_{\text{in}}}$ , where the constant is determined from matching with the earlier region. At large  $t$ , one expects linear growth with a constant rate  $\dot{y}_{\infty} = \sqrt{2/3}$  and with a small nonlinear correction:

$$y(t) = t\dot{y}_{\infty} + \delta_y(t).$$

Linearizing Eq. (B16) then gives

$$\delta_y(t) = -\frac{1}{2\dot{y}_{\infty}} \ln t + \text{const.}$$

In order to comply with the small time solution, the constant must shift the time by  $\ln(r_0 - 1)/\sqrt{r_{\text{in}}}$  so that one has

$$y(t) \sim \dot{y}_{\infty} \left( t + \ln \frac{r_0 - 1}{\sqrt{r_{\text{in}}}} - \frac{3}{4} \ln t + O(1) \right). \quad (\text{B17})$$

Returning to  $r(t)$  and solving the equation iteratively to find time, one obtains for  $r \gg \sqrt{r_{\text{in}}} \gg 1 \gg r_0 - 1$

$$t_{\text{gr}}(r_0, r) = \frac{r}{\dot{r}_{\infty}} - \ln \frac{r_0 - 1}{\sqrt{r_{\text{in}}}} + \frac{3}{4} \ln \frac{r}{\sqrt{r_{\text{in}}}} + O(1).$$

The constant  $O(1)$  was estimated as close to  $-0.6$  by subtracting the above asymptotic equation from numerical solutions of the RP equation at large  $r \sim 10^5$  for a variety of the  $r_0$  and  $r_{\text{in}}$  values. In order to obtain the incubation time, one then uses Eq. (14), which cancels the singularity at  $r_0 \rightarrow 1$ ; the result is presented in Sec. IV.

- 
- [1] K. F. Kelton and A. L. Greer, *Nucleation in Condensed Matter: Applications in Materials and Biology* (Elsevier, Amsterdam, 2010).
- [2] C. E. Brennen, *Cavitation and Bubble Dynamics* (Oxford Engineering Science Series, Oxford University, New York, 1995).
- [3] A. Megevand and A. D. Sanchez, *Phys. Rev. D* **77**, 063519 (2008).
- [4] A. Pullia, *Adv. High Energy Phys.* **2014**, 1 (2014).
- [5] S. Putterman, P. G. Evans, G. Vazquez, and K. Weninger, *Nature (London)* **409**, 782 (2001).
- [6] K. S. Suslick, N. C. Eddingsaas, D. J. Flannigan, S. D. Hopkins, and H. Xu, *Ultrason. Sonochem.* **18**, 842 (2011).
- [7] A. V. Neimark and A. Vishnyakov, *J. Chem. Phys.* **122**, 054707 (2005).
- [8] M. J. Uline and D. S. Corti, *Phys. Rev. Lett.* **99**, 076102 (2007).
- [9] D. I. Zhukhovitskii, *J. Chem. Phys.* **139**, 164513 (2013).
- [10] V. G. Baidakov and K. S. Bobrov, *J. Chem. Phys.* **140**, 184506 (2014).
- [11] J. Diemand, R. Angelil, K. K. Tanaka, and H. Tanaka, *Phys. Rev. E* **90**, 052407 (2014); **92**, 022401 (2015).
- [12] R. Angelil, J. Diemand, K. K. Tanaka, and H. Tanaka, *Phys. Rev. E* **90**, 063301 (2014).
- [13] T. T. Bazhiron, G. E. Norman, and V. V. Stegailov, *J. Phys. Condens. Matter* **20**, 114113 (2008).
- [14] Y. Cai, H. A. Wu, and S. N. Luo, *J. Chem. Phys.* **140**, 214317 (2014).
- [15] Ya. B. Zeldovich, *Acta Physicochim. URSS* **18**, 1 (1943).
- [16] K. Binder and D. Stauffer, *Adv. Phys.* **25**, 343 (1976).
- [17] H. Trinkaus, *Phys. Rev. B* **27**, 7372 (1983).
- [18] B. V. Deryagin, A. V. Prokhorov, and N. N. Tunitskii, *Zh. Eksp. Teor. Phys.* **73**, 1831 (1977).
- [19] A. V. Prokhorov, *Bull. Acad. Sci. USSR, Phys. Ser.* **239**, 1323 (1978).
- [20] V. A. Shneidman, *Sov. Phys. JETP* **64**, 306 (1986).
- [21] P. Hänggi, P. Talkner, and M. Borkovec, *Rev. Mod. Phys.* **62**, 251 (1990).
- [22] A. Umantsev, *Field Theoretic Method in Phase Transformations*, Lecture Notes in Physics, Vol. 840 (Springer, Heidelberg, 2012).
- [23] Occasionally, one talks about the diffusion of vacancies towards the cavity, which is similar to mass exchange. The resulting expression, however, is nonmacroscopic (in this sense “non-classical”) since it does not comply with the Navier-Stokes equation, being potentially relevant to smallest cavities with  $R \lesssim R_{\text{min}}$ .
- [24] M. Volmer, *Kinetics of Phase Formation*, Central Air Documents, 1966 (translated from German: Von Prof. Dr. M. Volmer, *Kinetik der Phasenbildung*, (Th. Steinkopff, Dresden and Leipzig, 1939).
- [25] A. D. Linde, *Usp. Fiz. Nauk* **144**, 177 (1984).
- [26] M. Volmer and A. Weber, *Z. Phys. Chem.* **119**, 227 (1926).
- [27] L. Farkas, *Z. Phys. Chem.* **25**, 236 (1927).
- [28] E. M. Lifshitz and L. P. Pitaevskii, *Physical Kinetics* (Pergamon, New York, 1981).
- [29] Some classical and nonclassical thermodynamic effects due to compressibility and volatility of the fluid are discussed, e.g., in Refs. [8, 11], in P. Debenedetti, *Metastable Liquids* (Princeton University, Princeton, NJ, 1996).

- [30] Yu. Kagan, *Russ. J. Phys. Chem.* **60**, 42 (1960).
- [31] In MD simulations, the Lennard-Jones fluid can be close to instability [8], while growth rates comparable to the speed of sound are observed [12].
- [32] L. D. Landau and E. M. Lifshitz, *Fluid Mechanics*, 2nd ed., Course of Theoretical Physics, Vol. 6 (Butterworth-Heinemann, Boston, 1987).
- [33] In the original Ref. [15] a dimensional estimation rather than an exact surface integral was used, without the numerical factor  $16\pi$ ;  $\tau$  equivalent to the one used in Eq. (3) was later introduced from the RP equation.
- [34] M. E. Fisher, *Physics* **3**, 255 (1967).
- [35] J. S. Langer, *Ann. Phys. (N.Y.)* **65**, 53 (1971).
- [36] J. D. Gunton, M. San Miguel, and P. S. Sahni, in *Phase Transitions and Critical Phenomena* edited by C. Domb and J. L. Lebowitz (Academic, New York, 1983), Vol. 8, p. 267.
- [37] M. Abramowitz and I. Stegun, *Handbook of Mathematical Functions* (Dover, New York, 1972).
- [38] V. A. Shneidman, *Sov. Phys. Tech. Phys.* **32**, 76 (1987).
- [39] V. A. Shneidman, *Sov. Phys. Tech. Phys.* **33**, 1338 (1988).
- [40] A. H. Nayfeh, *Introduction to Perturbation Techniques* (Wiley, New York, 1981), Chap. 12.
- [41] V. P. Skripov, *Metastable Liquids* (Wiley, New York, 1973).
- [42] O. Penrose, *J. Stat. Phys.* **89**, 305 (1997).
- [43] V. A. Shneidman, *Phys. Rev. E* **84**, 031602 (2011).
- [44] V. A. Shneidman, *J. Chem. Phys.* **141**, 051101 (2014).